Mathematical modeling of area under the curve assessment criteria to quantify the antioxidant and pro-oxidant capacity: Coffee extracts as a case study

M.A. Prieto[1*], J.A. Vázquez[1] and M.A. Murado

[1] Grupo de Reciclado y Valorización de Materiales Residuales (REVAL),
Instituto de Investigacións Mariñas (IIM-CSIC)
r/ Eduardo Cabello, 6. Vigo-36208. Galicia – Spain

*Corresponding author E-mail: michaelumangelum@gmail.com

Tel.: +34986214469; +34986231930
Fax: +34986292762

ABSTRACT

The development of a convenient mathematical application for testing the antioxidant and pro-oxidant capacity is essential in order to investigate potential sources of new agents and processes. In this regard, authors use the standardized values of the area under the curve of a kinetic profile of a dose-response agent, as a way to bypass the complex process of analyzing the kinetic variations of agents. In general, linear approaches are used, but such patterns frequently lead to unreliable results and misinterpretations, making it extremely difficult to compare the results from different assays. In this work, we have demonstrated the non-linearity of the dose-response area under the curve assessment criteria by means of simulations. A simple non-linear dose-response model was developed to describe the accurately response. As case study, experimental data of extracts of unroasted coffee beans from five different country-climate locations for the two most common coffee varieties (*Robusta* and *Arabica*) were obtained using the β-carotene and crocin bleaching *in vitro* assays. Their antioxidant capacity was analyzed in detail and compared with commercial standards. The results shows that the antioxidant capacity was greater than some of the commercial standards in terms of its maximum capacity, while when the analyses are based on rate parameters, the coffee extracts show between 6 to 40 times lower values than the standard antioxidants. In addition, to illustrate the advantages of using the standardized area units and the mathematical model developed, other more complex scenarios were recreated. We believe that the model application developed provides a simple alternative to summarize in meaningful parameters that characterize the response, it facilitates rigorous comparisons among the effects of different compounds and experimental approaches and it helps to comprehend multi-variable scenarios.

Keywords: antioxidant and pro-oxidant capacity; mathematical modeling; area under the curve, unroasted coffee beans.

Chemical compounds studied in this article: Linoleic acid (CID 5280450); β-Carotene (CID 5280489); Crocin (CID 5281233); 2,2'-Azobis(2-amidinopropane) dihydrochloride (CID 76344); butyl-hydroxyanisole (CID 24667); propyl 3,4,5-trihydroxybenzoate (CID 4947); butyl-hydroxytoluene (CID 15570435); 6-ethoxy-2,2,4-trimethyl-1,2-dihydroquinoline (CID 3293); 6-hydroxy-2,5,7,8-tetramethylchroman-2-carboxylic acid (CID 40634); (2R)-2,5,7,8-tetramethyl-2-[(4R,8R)-(4,8,12-trimethyltridecyl)]-6-chromanol (CID 14985); and (5R)-[(1S)-1,2-dihydroxyethyl]-3,4-dihydroxyfuran-2(5H)-one (CID 54670067).

NOMENCLATURE

Standards for testing the anti and pro-oxidant capacity:	
BHA	Butyl-hydroxyanisole.
ETX	Ethoxyquin.
BHT	Butyl-hydroxytoluene.
TOC	α-tocopherol.
PG	Propyl gallate.
Mn^{2+}	Manganese (II).
Hb	Hemoglobin.
Fe^{2+}	Iron (II).
Fe^{3+}	Iron (III).
Cu^{2+}	Cooper (II).
AAPH	2,2'-Azobis(2-amidinopropane) dihydrochloride.
AA	Ascorbic acid.
TBHQ	Tert-Butylhydroquinone.
TRO	Trolox.
Coffee extracts for testing the antioxidant capacity:	
C1	*Coffea arabica* from Australia.
C2	*Coffea arabica* from Nicaragua.
C3	*Coffea canephora robusta* from Cameroon.
C4	*Coffea arabica* from Guatemala.
C5	*Coffea canephora robusta* from Vietnam.
Others:	
AC	Antioxidant capacity.
M	Oxidation modifiers (anti- or pro-oxidant).
βC	β-carotene.
Cr	Crocin.
T	Temperature.
βCA	β-carotene assay.
CA	Crocin assay.
A	Antioxidant.
P	Pro-oxidant.
Traditional standardization of the area under the curve (Eq. (1) and Eq. (2)):	
AUC	Area under the curve.
t	Time (min).
i	Number of data measured along time.
R_i	Responses along time series.
Δt	The time interval of each measurement.
C	Control curve in the absence of M.
AUC_M	Area under the curve of M.
AUC	Area under the curve.
AUC_C	Area under the curve of C.
RAU	Relative area units.
r^2	Correlation coefficient
Model to describe the dose-time effect of M agents (Eq. (3), (4) and (5)):	

R	Response standardized in the format [0,1].
K	Asymptote.
τ	Substrate half-life ($R_{50\%}$).
α	Sigmoid shape parameter.
H_θ	Hyperbolic relation function for each parameter (θ=K, τ, α).
m_θ	Numerator parameter of the hyperbolic relation (θ=K, τ, α).
n_θ	Denominator parameter of the hyperbolic relation (θ=K, τ, α).
Standardization of the AUC responses (Eq. (6) and Eq. (7)):	
S	Substrate (µM).
S_0	Initial substrate (100 µM for the CA and 1 µM for βCA).
$\overline{P}$	Substrate protected (µM).
AOC_C	Area over the curve of the control.
Kinetic model for the standardized dose AUC responses (Eq. (8) and (9)):	
P_m	Maximum $\overline{P}$ (µM).
v_τ	Averaged rate parameter (µM $\overline{P}$/µM or µg M).
n	Percentage value of $\overline{P}$ (0-100%).
v_n	Rate parameter at n percentage value of R (µM $\overline{P}$/µM or µg M).
a	Sigmoid shape parameter (identical meaning of α in Eq. (3)).
Kinetic model for the pro-oxidant capacity of AAPH with T. Eq. (10) and (11):	
k	Rate constant chemical reaction.
k_B	Gas constant or the Boltzmann constant.
E_a	Activation energy (kJ/µM).
R	Constant of gases (kJ.µM/K).
Kinetic model for the antioxidant capacity of TRO with the pH (Eq. (12), (13) and (14)):	
$P_m^\bullet$	Asymptote or maximum $\overline{P}$ (µM of Cr protected).
τ_{Pm}	$\overline{P}_{50\%}$ (pH units)
c_{Pm}	Sigmoid shape parameter (identical meaning of α in Eq. (3)).
b	Slope (µM Cr.µM trolox^{-1}/pH)

1. INTRODUCTION

Studies have demonstrated that antioxidants have potential preventative effects against oxidative stress (Aruoma, 1999; Chatterjee, Poduval, Tilak, & Devasagayam, 2005; Gutteridge & Halliwell, 2010). Consequently, the search for naturally occurring compounds with antioxidant capacity (*AC*) has increased dramatically in the past years. Researchers have found many dietary sources of antioxidants such as cereals, fruits, oils, spices, vegetables and beverages (Carlsen et al., 2010; Faller & Fialho, 2009; Garcıía-Alonso, Pascual-Teresa, Santos-Buelga, & Rivas-Gonzalo, 2004; Lu, Yuan, Zeng, & Chen, 2011; Pellegrini et al., 2006; Pérez-Jiménez et al., 2008) that have proved disease-preventative and health-promoting effects counteracting most common oxidative processes, when they are added to the diet regularly. For the raw materials of beverages and in particular the unroasted coffee beans, little studies are available to consider them as source of alternative compounds (Madhava Naidu, Sulochanamma, Sampathu, & Srinivas, 2008; Ramalakshmi, Rahath Kubra, & Jagan Mohan Rao, 2008).

However, before any information is provided, much attention must be paid to the way of computing the equivalent *AC*. Consistently, the *in vivo* and *in vitro* methods, to test new promising sources of antioxidants, are based on a single concentration at one time, expecting that those single values will be equal at any lower or higher concentration at any time (as a linear behavior). In fact, this pattern only takes place in particular cases, because the oxidation reactions in which antioxidants and pro-oxidants (hereafter oxidation modifiers: *M*) are involved are complex. The nature of the *M*, the substrate and the environment, as well as the involved mechanism, are factors which can perturb significantly the oxidation process (Frankel, 1994; Hamilton, 1997; Laguerre, Lecomte, & Villeneuve, 2007). Perhaps, one of the causes that force researchers to use simplistic quantification procedures is the lack of a universal method, capable of assessing the *AC* independently from the system under study. In consequence, it has become essential to test the compounds with different methods, and as a result, authors tend to simplify the calculation method in order to amplify the number of testing procedures. Despite the advisability of using mechanistic or empiric kinetic models as indicated by different authors (Murado & Vázquez, 2010; Özilgen & Özilgen, 1990; Prieto, Murado, Vázquez, & Curran, 2014; Ragnarsson & Labuza, 1977; Terpinc, Bezjak, & Abramovič, 2009; Wardhani, Fuciños, Vázquez, & Pandiella, 2013), researchers continue to use simple calculation tools more often than necessary. However, the method used to measure and compute the antioxidant capacity has a major impact on the results due to the complexity of oxidation reactions in both, *in vivo* and *in vitro*.

The detailed mechanistic description of oxidations is complex (Ragnarsson & Labuza, 1977) and varies from one to the other systems (Thomas, Chen, Franklin, & Rudel, 1997), which has led to the search for empirical general models, able to describe the most common profiles. For example, the power function developed by Terpinc, Bezjak, & Abramovič (2009) is appropriate only to adjust fractional-order kinetic profiles, but fails in the description of first-order processes or sigmoidal profiles. Other empirical approaches such as the Logistic and Weibull equations, have been transferred from other fields to describe the oxidation action (Murado & Vázquez, 2010; Özilgen & Özilgen, 1990; Wardhani et al., 2013), but are rarely used. From those equations, researchers are able to produce key parameters to summarize the responses, such as the asymptote, maximum velocity or the lag-phase. They can characterize the response and help to quantify the effect of *M* agents. In general, the three parameter sigmoidal group of functions (such as the Logistic, Weibull, Hill, Gompertz or Richards-Chapman) is the best solution to fit individually the kinetic profiles corresponding to a series of increasing levels of *M* agents. Alike in many other complex systems (De Lean, Munson, & Rodbard, 1978), some authors (Gieseg & Esterbauer, 1994; Prieto, Murado, Vazquez, Anders, & Curran, 2013) have suggested directly or

indirectly further analysis, in which the oxidative responses are described as a function of both the dose and the exposure time, in a bi-variate form.

Alternatively, the area under the curve (*AUC*) of a kinetic profile of a dose-response agent has become routinely applied for many antioxidant analytical procedures (Dávalos, 2004; Huang, Ou, Hampsch-Woodill, Flanagan, & Deemer, 2002; Naguib, 2000). Its advantages are: a) simplicity, because it simplifies one variable and allows to assess complex scenarios with simple relations; and b) applicability, because it can be used in almost all procedures and types of responses. Its weakness is the lack of an established mathematical model to describe the *AUC*. In the best-case scenario, authors describe the dose-response in linear terms, which frequently leads to unreliable results and misinterpretations, making it extremely difficult to compare the results from different assays.

In this work, firstly, the non-linearity of the dose-response of the *AUC* of kinetic profiles by means of simulations is demonstrated. Secondly, a simple non-linear dose-response model was developed to describe them and applied as a general tool to test the effectiveness of compounds. The model was experimentally tested on two well-known *in vitro* competition assays, the β-carotene (βC) and crocin (Cr) bleaching asymptotic reactions (Prieto et al., 2013), appropriate for lipophilic and hydrophilic matrices, respectively. As a natural agent case study, the dose-time dependency of extracts of unroasted coffee beans from five different country-climate locations for the two most common coffee varieties (*Robusta* and *Arabica*) were used, and their capacity were compared with commercial standards of antioxidants. The illustration of the capabilities of the approach summarizes the kinetic responses in a very consistent way. The interactions produced by different agents (anti- or pro-oxidant) as function of different environmental factors (such as *pH* or *T*) are analyzed. Finally, the model was verified for other relevant methods, using available experimental data from the bibliography.

2. MATERIALS AND METHODS

2.1. Kinetic β-carotene and crocin bleaching assays

The β-carotene assay (βCA) (Marco, 1968) and crocin assay (CA) (Bors, Michel, & Saran, 1984) are two widespread methods for the *AC* evaluation that shares analytical similarities, and at present, their procedures are detailed reviewed (Prieto et al., 2013; Prieto, Rodríguez-Amado, Vázquez, & Murado, 2012):

2.1.1. Reagents and reaction conditions

βCA: Two mg of βC (1 μM in the final reaction), 0.25 mL of linoleic acid and 2 g of Tween-40 were dissolved in 20 mL of chloroform, vigorously mixed and the chloroform is evaporated (40 °C/~15 min). To the resulting oily residue 300 mL of buffered Mili-Q water (100 mM Briton, pH=6.5) at 45 °C was added. The absorbance at 470 nm of the reagent prepared was ~1.40.

CA: Four mg of Cr (100 μM in the final reaction) and 75 mg of 2,2'-Azobis(2-amidinopropane) dihydrochloride (AAPH, 7.68 mM in the final reaction) were dissolved in 25 and 5 mL, respectively, of 100 mM Briton buffer, pH=5.5, in Mili-Q water at 40 ºC. The absorbance at 450 nm of the reagent prepared was thus ~1.40.

2.1.2. Procedure

The procedure was performed by adding 50 μL of sample and 250 μL of reagent into the wells (350 μL) of a microplate of 96 units (Thermo Scientific Nunc 96-Well Polypropylene MicroWell

Plate with flat bottom). The microplate-reader (Multiskan Spectrum Microplate Photometers from Thermo Fisher Scientific) was programmed to 45°C for the βCA and 37 °C for the CA with agitation reading the absorbance at intervals of 3, 5 and 10 minutes (initiation, propagation and asymptotic phase), during a period of 200 minutes (total of 30 measures). The antioxidant standards and samples were analyzed kinetically for eight different doses previously ranged. All standards and samples were dissolved in water:ethanol (9:1).

2.1.3. Traditional standardization of the area under the curve

A simple approach to characterize the antioxidant (*A*) action through a single value is achieved by calculating the area under the kinetic profile (Dávalos, 2004; Huang, Ou, Hampsch-Woodill, Flanagan, & Deemer, 2002; Naguib, 2000). Also, it has been applied in more complex responses to simplify the variable time response to one value (Prieto, Murado, & Vázquez, 2014). The response is defined in terms of area under the curve (*AUC*) that can easily be calculated by any numerical integration method (Pruessner, Kirschbaum, Meinlschmid, & Hellhammer, 2003; Schisterman, Faraggi, Reiser, & Trevisan, 2001; Stephen, Stevens, & Chaturvedi, 2000), such as the trapezoidal rule as follows:

$$AUC = \frac{R_1 \Delta t_1}{2} + \sum_{i=2}^{i=n-1} R_i \Delta t_i + \frac{R_n \Delta t_n}{2} \quad (1)$$

where *i* is the number of data measured along time *t, R_i* are the responses along an arbitrary time series and *Δt* is the interval of each measurement. The *AUC* in the presence of an antioxidant, decreases and in the presence of a pro-oxidant (*P*) agent increases, in both cases asymptotically. For the particular case here analyzed, the area values represent the accumulative amount of substrate bleached during the total time (*t*) analyzed. Then, the *AUC* responses of a dose-response of an *M* agent are standardized in relation to *AUC* obtained for the control, which leads to the formulation of the relative area units (*RAU*) as defined by other authors (Dávalos, 2004; Huang, Ou, Hampsch-Woodill, Flanagan, & Prior, 2002; Naguib, 2000) as follows:

$$RAU\left(M\right) = AUC_C - AUC_M \quad (2)$$

where AUC_C and AUC_M are the area units corresponding to the kinetic profiles found in the absence (*C*, control) and presence of an *M* agent concentration, respectively. The physical meaning of the *RAU* responses in the experimental assays here analyzed would correspond to the accumulative substrate protected for the total time of the assay (μM.min) by a given *M* agent concentration. The *RAU* standardization proved to be a highly robust criterion, able to summarize in a single and direct datum the global feature of any kinetic profile.

2.2. Standard *M* compounds for an illustrative analysis

2.2.1. Antioxidants

(a) Butyl-hydroxyanisole (BHA): a synthetic food additive (E320) mainly used as an antioxidant and preservative. Its known capacity is suitable in lipophilic and hydrophilic environments.
(b) Butyl-hydroxytoluene (BHT): a synthetic lipophilic (fat-soluble) organic compound, chemically a derivative of phenol, which is useful for its antioxidant properties. It is primarily used as a food additive (E321).
(c) Propyl 3,4,5-trihydroxybenzoate or propyl gallate (PG): an antioxidant that has been added to foods containing oils and fats to prevent oxidation (E310).

(d) (2R)-2,5,7,8-tetramethyl-2-[(4R,8R)-(4,8,12-trimethyltridecyl)]-6-chromanol or α-tocopherol (TOC): a natural fat-soluble organic compound (E306) consisting of various methylated phenols (a type of tocopherol or vitamin E), that is useful for its antioxidant properties.
(e) 6-ethoxy-2,2,4-trimethyl-1,2-dihydroquinoline or ethoxyquin (ETX): commonly used as a food preservative (E324) in pet foods to prevent the rancidification of fats, in spices to prevent color loss due to oxidation of the natural carotenoid pigments and as a pesticide.
(f) L-hexuronic acid (vitamin C) or Ascorbic Acid (AA): a naturally occurring hydrosoluble organic compound with antioxidant properties. Ascorbic acid and its sodium, potassium, and calcium salts are commonly used as antioxidant food additives (E300-304)
(g) Tert-Butylhydroquinone (TBHQ): It is a derivative of hydroquinone, substituted with tert-butyl group. TBHQ is a highly effective antioxidant in foods (E319). It is added to a wide range of foods, with the highest limit (1000 mg/kg) permitted for frozen fish and fish products.
(h) Manganese sulfate (Mn^{2+}): a required trace mineral for all known living organisms, also extensively present as possible interference in salts may be able to act as a metal chelator (e.g., iron-sequestrants) and inhibit Fenton-type reactions that produce hydroxyl radicals through complexation/chelation reactions.
(i) 6-hydroxy-2,5,7,8-tetramethylchroman-2-carboxylic acid (Trolox, Tr): A water-soluble analog of vitamin E used in biological or biochemical applications to reduce oxidative stress or damage.

The concentration ranges in μM of the *A* used for the βC reaction are: BHA: 0-(0.5)-5, BHT: 0-(3)-30, ETX: 0-(0.0004)-0.004, TOC: 0-(0.004)-0.04, PG: 0-(8)-80. The concentration ranges in μM of the antioxidants used for the Cr reaction are: AA: 0-(30)-300, ETX: 0-(3)-30, Tr: 0-(15)-150, TBHQ: 0-(80)-800, Mn^{2+}: 0-(12.5)-125. All compounds were purchased from Sigma S.A. (St. Louis, MO, USA).

2.2.2. Potential pro-oxidant agents

(a) Iron (II) and Iron (III) sulfide (Fe^{2+}, Fe^{3+}): much attention has been paid to its oxygen complexes (ferryl and perferryl radical) in the food industry as they are considered as primary catalysts (initiators) of lipid peroxidation in meat products and others that contain lipids.
(b) Porcine Hemoglobin (Hb) in reduced form (Fe^{2+}): the iron-containing oxygen-transport metalloprotein in the red blood cells. Hb can be found in many food compounds interfering with its antioxidant capacity and also is a typical compound that caused rapid rancidity.
(c) Copper (II) sulfate (Cu^{2+}): an essential trace nutrient to all higher plant and animal life, also widely present in biological extracts, water and as possible interference in salts.
(d) AAPH: a hydrophilic chemical compound used to study the chemistry of the oxidation of drugs or the capabilities of antioxidants in different system reactions.

The concentration ranges in μM of the pro-oxidants used for βCA are: Fe^{2+} 0-(1.5)-15; Cu^{2+} 0-(15)-240; Hb 0-(2)-20.0. For CA, AAPH 0-(12.5)-125 was used. All compounds were purchased from Sigma S.A. (St. Louis, MO, USA).

2.3. Compound extraction and preservation of coffee samples

A set of five unroasted coffee beans, free of additives (especially the antioxidant ones), were freely provided by local manufacturer (CAFÉS CAMPINAS S. PAULO). Beans were harvested in 2013 at different locations from two different varieties: (C1) *Coffea arabica* from Australia; (C2) *Coffea arabica* from Nicaragua; (C3) *Coffea canephora robusta*, caracolillo selection, from Cameroon; (C4) *Coffea arabica* from Guatemala; and (C5) *Coffea canephora robusta* from Vietnam.

The coffee beans were grounded to obtain a homogeneous fine powder (<0.5 µm) and extracted in water in an autoclave (Almajano, Carbó, Delgado, & Gordon, 2007; Perva-Uzunalić et al., 2006). The extractions were performed in duplicate. Four consecutive autoclave extractions with 100 mL of distilled water at 105 ºC for 60 min were applied to 10 g of each sample. The extracted material was centrifuged several times and the supernatant was filtered through GF/D (2.7 µm) and GF/F (0.7 µm) glass microfibre filters (Whatman®), lyophilized and preserved at -20 ºC. In all cases, the concentration ranges in g/L in the final solution used were: 0-(0.05)-0.5 for the CA and 0-(0.03)-0.3 for the βCA.

2.4. Numerical and statistical methods

Fitting the experimental results to the proposed equations was carried out in two phases. First, parametric estimates were obtained by minimization of the sum of quadratic differences between observed and model-predicted values, using the nonlinear least-squares (quasi-Newton) method provided by the macro *Solver* de *Microsoft Excel* 2003 spreadsheet (Kemmer & Keller, 2010). It allows quick testing of hypotheses and display of its consequences. Subsequently, the determination of the parametric confidence intervals and model consistency (Student´s *t* and Fisher´s *F* tests, respectively, in both cases with $\alpha = 0.05$) were calculated using the '*SolverAid*' macro (Prieto, Vázquez, & Murado, 2012; Prikler, 2009) freely available from de Levie's web site (http://www.bowdoin.edu/~rdelevie/excellaneous/). The *'SolverStat'* macro (Comuzzi, Polese, Melchior, Portanova, & Tolazzi, 2003), freely available from Polese's web site (http://www.freewebs.com/solverstat/solverstat/solverstat.htm), was used for detecting possible anomalies in the distribution of parametric estimates and residuals.

3. RESULTS

At first, we will illustrate the non-linearity of the relative area units. Afterwards, a mathematical model will be proposed and applied, as an example, to *A* and *P* experimental data values. Then, the analytical procedure is applied to several commercial standards and to the obtained coffee extracts for the two complementary assays (βCA and CA). Finally, to illustrate the capabilities of the model, the analysis was extended to the combined kinetic effect of the main system variables (*pH* and *T*) and the effect of an *A* and a *P*, simultaneously.

3.1. Illustration of the non-linearity of the area under the curve

The oxidant action implies interfering in an autocatalytic process in which no less than four chemical species are present (oxygen, oxidizable substrate, antioxidants and oxidation products), reactions of first and second order can take place and interactions can occur at several levels of the sequence. When the *RAU* values or similar standardizations of the *AUC* are plotted against the dose-response of an agent *M*, typically authors use for their analysis linear relations, but as would be here discussed, such a restricted behavior only occurs in very specific situations. Furthermore, instead of comparing the linear dose-responses between each other, the common practice is to use the dose-response of one commercial antioxidant as a calibration curve to compute the equivalent antioxidant capacity of a sample which is only tested at one single-dose, assuming several uncertain aspects as correct.

Murado & Vázquez (2010) developed a general model to describe the dose-time effect of *M* agents and afterwards, other authors (Prieto, Rodríguez-Amado, et al., 2012) extended its application into more specific cases. The model is based on the accumulative Weibull distribution (Weibull & Sweden, 1951) to describe satisfactorily the time part of the profile as follows:

$$R = K\left\{1-\exp\left[-\ln 2\left(t/\tau\right)^{\alpha}\right]\right\} \quad (3)$$

where R is the response obtained to reproduce possible patterns of an A, K is the asymptote, τ is the substrate half-life or time when 50% oxidation is achieved ($R_{50\%}$), and α is a shape parameter associated with the slope of the profile and can produce potential profiles when $\alpha<1$, first order kinetic ones when $\alpha=1$ and a variety of sigmoid profiles when $\alpha>1$. The dose-effect is described as saturable type effect (Gieseg & Esterbauer, 1994) by the following hyperbolic (H) relation function:

$$H = \left(1+m\cdot M\right)/\left(1+n\cdot M\right) \quad (4)$$

where the pairs m and n are fitting coefficients. To describe the effect as a time-dose process, authors modified each parameter (θ) of Eq. (3) by the hyperbolic relation in Eq. (4) as follows:

$$R\left(t,M\right) = K\cdot H_K\left\{1-\exp\left[-\ln 2\left(\frac{t}{\tau\cdot H_\tau}\right)^{\alpha\cdot H_\alpha}\right]\right\} \quad \text{with} \quad H_\theta = \left(1+m_\theta\cdot M\right)/\left(1+n_\theta\cdot M\right) \quad (5)$$

where the θ subscript represents the modified parameter (K, τ or α). The individual coefficients m_θ and n_θ lack of proper meaning, but jointly they define a term as a function of the concentration of a given M. If any of the parameters of Eq. (4) (m or n) are equal to zero, the modified equation of the parameters would be a linear one (increasing or decreasing respectively) and if $m\neq n\neq 0$, the function would be a hyperbolic one. The solution has been proved to work in many different scenarios.

Therefore, if we assume that this time-dose response model describes appropriately the oxidation process –in accordance with experimental results– by simulating time-dose-dependent responses, we could test the behavior of the *RAU*, in all circumstances, and thus discuss the problems and appropriate methods to analyze the *RAU* dose-responses.

Several aspects need to be highlighted regarding kinetic behavior of agents to illustrate completely the general non-linearity of the *RAU* values: 1) the variations of the profiles as function of the dose of an agent; 2) the experimental definition of the curves (initial, propagation and asymptotes) in the 2D frame of the response and/or the range of concentrations tested; and 3) the presence of one common asymptote or asymptotic variances as a function of the dose of the agent under analysis. Figure 1 and Table 1 show the illustrations and parametric values of six clarifying simulations (Cases 1 to 6, two for each of the previously highlighted points). Each case is divided in two figures (a and b). The first one (a) shows the responses (R, from 0 to 1 units) for each of the kinetic profiles (0-200 units) of increasing concentrations of an agent M (0-100 units). Note that the control profile has thicker line than the simulated increasing concentrations of M. The second one (b) shows the *RAU* values obtained.

Figure 1 (part A, cases 1 and 2), displays these cases related to the specific profile variations. A first-order kinetic profile is supposed (in Eq. (5) $\alpha=1$ and $m_\alpha=n_\alpha=0$) and for the dose-response pattern the half-life parameter (τ) is modified by means of a linear increasing relation (case 1, $m_\tau\neq 0$ and $n_\tau=0$) and by an asymptotic increasing relation (case 2, $m_\tau=0$ and $n_\tau\neq 0$). In both cases, even for the linear one, the *RUA* values are non-linear. If we focus on the concentration ranges below 25 units, a linear relation could be assumed. As it is shown in Figure 1 (part B, case 3), such linear relations of the *RUA* values exist only in the specific scenery, in which the kinetic

profiles for all the doses are defined for one common asymptote (K=1) and the half-life parameter (τ) is extended by means of an increasing linear relation (m_τ=0 and $n_\tau \neq 0$). To produce such a case, only 25% of the possible area of the 2D response of the graph is fulfilled. If we would be analyzing the profiles by mathematical models, we would agree that the definition of the curves must be complete, but as we are summarizing the profile by its standardized *AUC* values, focusing only on the 25% of the possible 2D response, seems to be a restriction. Thus, when the concentration range of case 3 is expanded, as shown in case 4, the area units become clearly non-linear, even in the only scenario in which they would be a linear one. Additionally, when analyzing the oxidations and their kinetic inhibition, many responses (such as those produced in the DPPH method and similar) show different asymptotes for each dose. Figure 1 (part C, case 5) shows the same kinetic profiles produced by case 3 but adding a parameter that modifies the final asymptote. Such a pattern confirms that even when the curves are well defined to be linear, they have to end in a common asymptote, because otherwise it causes inevitable non-linear *RAU* responses, no matter what range of concentrations are used or what mode of profiles are involved. Finally, Figure 1 (part C, case 6) exemplifies the weakness of using the standardized *AUC* responses. As it can be observed, the dose responses obtained for case 6 and case 1 are identical, but their kinetic patterns are completely different. Case 1 extends linearly the half-life parameter ($m_\tau \neq 0$ and n_τ=0) and case 6 reduces the asymptote (K) non-linearly (m_K=0 and $n_K \neq 0$). When using the area units, we are able to simply quantify the responses, but we are neglecting the mechanistic patterns behind, which could cause serious problems, if they are not well understood.

In general, for any simulated type of kinetic profiles, the dose-response in terns of *RAU* or any other way of defining the *AUC* values are non-linear, and the use of linear approaches will always produce unsatisfactory solutions. Therefore, a mathematical tool, that allows summarizing the dose-response in simple guiding values, is proposed next.

3.2. Mathematical modeling of the dose-response area units of compounds

Before any model is proposed, the traditional ways for standardizing the *AUC* into *RAU* values must be slightly modified.

3.2.1. Standardization of the AUC responses

The way that the *AUC* responses are standardized in terms of *RAU* values (Eq. (2)) are only useful for the definition of dose-responses of *A* agents, because the *AUC* decreases as a function of increasing concentration of an *A* and increases as a function of a *P*. In addition, the *RAU* values lack of useful physical meaning. Therefore, before any model is considered the standardization of the responses must be changed. For the case of the experimental responses here tested, the best solution is to rearrange the *AUC* as a function of the concentration of an *M* agent in terms of the substrate (S) protected ($\overline{P}$). Therefore, for an antioxidant, the definition should be as follows:

$$\overline{P}(A) = S_0\left(\frac{AUC_C - AUC_M}{AUC_C}\right) \tag{6}$$

in which S_0 is the initial substrate concentration in µM used for the analytical procedures tested (for the CA the S_0 value is equivalent to 100 µM of Cr and for the βCA to 1 µM of βC) and the other terms remain as in Eq. (2). The relation considers that AUC_C is the maximum response possible and the responses are thus standardized. However, when standardizing the responses for *P* agents, the maximum possible pro-oxidizing area is the area over the curve of the control

(AOC_C). Therefore, the response of the substrate protected ($\overline{P}$) as a function of a P agent must be performed as follows:

$$\overline{P}(P) = S_0\left(\frac{AUC_C - AUC_M}{AOC_C}\right) \tag{7}$$

When the M agent is an antioxidant, the $\overline{P}$ value will be a positive one, and when it is a P will be a negative one. Additionally, by standardizing the response in relation to the control, the results obtained are less dependent on the experimental conditions, particularly on the initial concentration of the reactive species, which is in practice, one of the common problems when analyzing the efficacy of an antioxidant and a potential cause of inaccurate results (Balk, Bast, & Haenen, 2009). For other analytical scenarios the internal specific meanings of the responses must be different, but the relations should be kept.

3.2.2. Dose-response model

Data obtained in the βCA are used to illustrate the procedure to assess the capacity of agents of opposite effects. Figure 2A shows the illustrative application of those standardizations to analyze the antioxidant effect of BHA and the pro-oxidant of Hb as a function of time and dose. Figure 2 (A1 and A3 plots) shows the raw dose-time response obtained by βCA, in which the black dots (●) are the results for the control values and the other dots are the responses for increasing concentrations of the agents. The white dots (○) in Figure 2 (A2 and A4 plots) represents the standardized $\overline{P}$ values obtained by the kinetic dose-responses showed in Figure 2 (A1 and A3).

The characteristic asymptotic variation of $\overline{P}$ as function of most agents suggests that some radical-generating property of the system can be saturated (Gieseg & Esterbauer, 1994). This type of dose-response patterns, in general, can be adjusted by a group of mathematical expressions (mechanistic or not) that translates the pattern of the response into parameters that allow to deduce the meaning and/or quantify the effect of the dependent variable in a simple and global mode. Among the most common, hyperbolic, potential or sigmoid functions are traditionally used in biological systems due to their manageability. Although if we generalize the action in 2D-frame, those models that cover the maximum possible responses and minimize the number of parameters, even if the availability of mathematical expressions is significant, the group that best meets these conditions and had been applied in different fields with high level of accuracy, is the group of sigmoid functions. In general, the three parameter sigmoid group of functions (such as the Logistic, Weibull, Hill, Gompertz or Richards-Chapman) is the best solution to fit individually the $\overline{P}$ values corresponding to a series of increasing levels of M agents. After testing those models, the same one described previously (Eq. (3)), was found to be the most satisfactory with the highest level of accuracy. Thus, the dose-response of $\overline{P}$ values can be fitted to the following equation rearranged for our own purposes:

$$\overline{P}(t,M) = P_m\left\{1-\exp\left[-\ln(2)^{1-a}\left(\frac{2v_\tau}{P_m a}M\right)^a\right]\right\} \tag{8}$$

The parameter P_m is the averaged maximum substrate protected, asymptotic value of the response (μM of βC and Cr in this case), which is specific of each M agent. The parameter v_τ corresponds to the amount of molecules protected per unit of M (μM of the protected substrate/μM of M) at the agent concentration that produces the half-maximal response ($\tau = P_m/2$), which is the value of maximal predictability, because it corresponds also to the average

molecules of substrate protected per molecule of *M* agent. The parameter *a* remains with the same shape profile meanings as described in Eq. (3) for the parameter α. When the *M* agent is a *P* the parameter P_m will be negative and when it is an *A* will be a positive one.

In addition, if the specific amount of molecules protected per unit of *M* at any given percentage *n* of the response is desired, it can be computed simply by rearranging the Eq. (8) as follows:

$$\overline{P}(t,M) = P_m \left\{ 1 - \exp\left[-\ln(1-0.01n)^{1-a} \left(\frac{2v_n}{P_m a} M \right)^a \right] \right\} \quad (9)$$

in which *n* can be any value between 0-100%, consequently the corresponding v_n (μM of the protected substrate/μM of *M*) can be computed to obtain any *n* percentage of the maximum μM of the substrate protected P_m. Other parameters of Eq. (9) remain with the same meaning as in Eq. (8).

For the illustrative responses assessed in Figure 2 (part A), all the parametric values are presented in Table 2, showing lower confidence intervals (α=0.05) and higher correlation coefficients in all cases (r^2>0.99), thus demonstrating the precision of this approach.

3.2.3. Comparison criteria for potential equivalent capacity determination

Consequently, we can consider in two meaningful ways to compare *M* activities. The first one would consist of plotting the specific $\overline{P}$ variations given by Eq. (8) as a function of the agent concentration. It will provide an efficient way to determine graphically the equivalent potential capacity of samples. This can provide a fixed value, which allows the visualization of the agent-specific dynamics of these effects (positive for *A* and negative for *P*) as shown in Figure 2 (A2 and A4 plots). The other one would be based on the combinatory information provided by the numerical values of the parameters P_m and v_τ of Eq. (8). These values can be used to compare the activities of different *M* agents. For example, the P_m parameter of BHA showed that the maximum capability is to protect 0.77 μM βC protected (or 77 %), on the other hand, the v_τ showed that one molecule of BHA protects as an average 0.271 molecules of βC (0.271 μM βC protected/μM of BHA). The information provided by the combination of both values represents a robust tool to compare the activities of different antioxidant agents based on the parametric estimations time-dose response. Authors may only focus in one parameter, depending on their interests, for example the maximum protective capabilities or the average amount molecules protected per molecule of *M* agent. In any case, with both values, an intuitive solution to compare *M* activities of compounds by a mathematical analysis is obtained, offering researchers a simple solution based on parametric non-linear values to assess *M* action and compare their capacity rigorously.

In both cases, graphically or numerically, the responses are effectively summarized in a time and dose form. Therefore, the potential equivalent capacity of samples and standard antioxidants and pro-oxidants can be compared effortless. Furthermore, the application may facilitate the ranking process and the selection of appropriate concentrations of natural products to replace commercial antioxidants, as we shall see next.

3.2.4. Application to assess and compare lipophilic and hydrophilic standard antioxidants and pro-oxidants

The previous standardizations and mathematical modeling was applied to the individual chemical entities (antioxidants and pro-oxidants) described in the material and methods section

in both experimental reactions (βCA and CA, representative of lipophilic and hydrophilic environments, respectively). All the kinetic dose-response results are shown in Figure A1 (Appendix section). Figure 2 part B, C and D, shows the standardized $\overline{P}$ values obtained (dots ○) and the fittings to Eq. (8) (lines) for all the tested agents.

In general, the antioxidant quantity needed to counteract the hydrophilic radicals produced by the degradation of AAPH molecules are less effective than those found to counteract the lipophilic radicals produced by the oxidation of linoleic acid (Table 2). Eq. (8) describes accurately all the dose responses studied (Table 2). Using numerical values of the parameters P_m and v_τ of Eq. (8) as assessment criteria (Figure 2, part E), the following order of activities can be established for each of the reactions:

a) For βCA the antioxidant potential would be as: *ETX* > *BHA* > *BHT* > *TOC* > *PG* > Mn^{2+}. The pro-oxidant order would be as: Hb > Fe^{2+} > Cu^{2+} > Fe^{3+}.

b) For CA the antioxidant potential would be as: *ETX* >*TRO* > *PG* > *AA* > *TBHQ*.

In addition, as a prove of accuracy of the approach here discussed, the amount of reduced hemoglobin used, which refers to hemoglobin (considering an average of 64,500 Da per molecule) which contains iron in the Fe^{2+} oxidation state, had approximately the same quantity of Fe^{2+} as the amount introduced directly as iron (II) sulfide. The graphical representation of the results (Figure 2, plot A4 for Hb and plot D1 for Fe^{2+}) are approximately equivalent. In fact, the parametric response (Table 2) shows nearly identical P_m and a parameters. The v_τ parameter, which is the only one related to the molarities of the agent, shows that Hb was 62,125 times higher than the one obtained as Fe^{2+}. Value highly concordant with the average estimated molecular weight of Hb, demonstrating the reliability of the tools here developed.

3.3. Application to assess the antioxidant capacity of natural agents: Coffee extracts as a case study

None of the bleaching kinetics of the tested compounds, in the absence of linoleic acid or AAPH, differed significantly from the control. In Table 2 and Figure 3 we present the results of the proposed approach to extracts of unroasted coffee beans from five different country-climate locations for the two most common coffee varieties (*Robusta* and *Arabica*). Figure 3 (part A) shows the dose-time dependency results of the five coffee samples (C1 to C5) for the two complementary assays (βCA and CA). The dose relations used are specified in the material and methods section. From a general view, only slighted differences can be perceived.

When we summarize the dose-responses in terms of the standardization described by Eq. (6) and the $\overline{P}$ dose-responses are computed using Eq. (8), always satisfactory solutions are achieved. The fitting parameters obtained, the parametric statistical estimations and correlation coefficients of determination (r^2) are presented in Table 2. *AC* of coffee extracts was compared in detail with commercial standards of antioxidants by means of the graphical and numerical criteria (Figure 3, B and C plots).

Based on the behavior profile (graphical criteria, Table 2, Figure 3 plots B1 and C1), the capacity of the coffee extracts can be followed as function of its concentration and compared to the responses of common commercial antioxidants. To simplify the comparison process, both the dose-responses of coffee extracts and the commercial antioxidants are expressed in µg of the compound in the reaction for the lipophilic and hydrophilic assessed environments. Exceptionally, for clarification, ETX and TOC antioxidants in B1 plot of Figure 3 is expressed as $x10^{-2}$ and $x10^{-1}$ µg. This graphical representation (the most simple and visual way) to analyze the

parametric non-linear response of the antioxidant equivalent action and comparing their capacity rigorously, provides an easy tool that facilitates the selection of appropriate concentrations of natural products to replace commercial antioxidants. Therefore, the non-linear equivalent responses of natural antioxidant compounds are characterized and compared with commercial substances within the concentration range tested. Thus, the potential equivalent capacity can be computed easily. For example, the following *in vitro* results can be concluded:

-In lipophilic environments, ~45 μg of C4 (*Coffea arabica* from Guatemala) is equivalent to ~8 μg of BHT.

-In hydrophilic environments, ~25 μg of C4 (*Coffea arabica* from Guatemala) is equivalent to ~2.6 μg of Trolox.

Using numerical values of the parameters P_m and v_τ of Eq. (8) as assessment criteria (Table 2, Figure 3, B2, B3, C2 and C3 plots), the differences are narrow and were much higher in a hydrophilic environment than in a lipophilic one. Based on the numerical parameter value P_m, at a given concentration (that can be found by using Eq. (9)), all coffee samples are able to counteract between 70-80 % of the oxidation of the Cr and βC substrates. Those values are greater than some of the standard antioxidants. When the analyses are based on the v_τ parameter, the coffee samples show between 6 to 40 times lower values than the standard antioxidants.

Beyond quantitative differences, all the coffee samples promote the antioxidant capacity in both lipophilic and hydrophilic environments. However, researchers must keep in mind that the equivalent potential capacity of coffee extracts reported in this study is only valuable for *in vitro* responses. Thus, if any of these natural extracts were required to replace commercial antioxidants, the *in vitro* responses found only serves as guiding values of the real responses that may be found for "*in vivo*" assessments.

3.4. Extension of the model application to the combined effect of system variables, antioxidant and pro-oxidant agents

In addition, we have extended the analysis to some aspects that reveal the capacity of the proposed approach to simplify responses for describing the interactions produced by different factors in a very consistent way. In the food industry, as well as other related areas, it is interesting to analyze the capacity (*A* or *P*) behavior of compounds (standards, natural products, complex matrix, etc) as function of different environmental factors (such as *pH* or *T*). As example, we have selected the CA and experimentally formulated the following tri-variate interactions: a) the time course of the reaction, the *P* action (using AAPH) and the temperature; and b) the time course of the reaction, the *A* action (using trolox) and the *pH*.

The advantage of applying the area units is that it simplifies one variable (*t* in this case) and allows with simple relations to assess more factors than other alternative methods. In those complex scenarios, many different responses are found. Thus, to be able to include the environmental factor into the previous developed model (Eq. (3)) and to correctly interpret the results, simultaneous description of all curves must be used, rather than fitting each one individually (De Lean et al., 1978).

3.4.1. Kinetic assessment of the P capacity of AAPH with temperature.

The kinetic response in the CA for four temperatures (32, 37, 40 and 45°C) where studied in the presence of eleven AAPH concentrations (range: 0-20.5 mM). All the resulting kinetic profiles (Figure 4, part A) could be described with accuracy and simplicity by simplifying the kinetic part

of the response in terms of the averaged substrate protected $\overline{P}$ for each temperature (dots of Figure 4, plot B1 and numerical parameters in Table A1). As expected, the temperatures effect (in the range studied) only perturbs the values of v_τ increasing its value as function of *T*. However, the possibility to incorporate the effect of temperature as a third variable into Eq. (8), requires to use the Arrhenius model. Briefly, the Arrhenius equation establishes that the rate constant (*k*) of a chemical reaction is a function of the absolute temperature (*T* in Kelvin degrees) according with:

$$k = k_B \exp\left(-E_a / RT\right) \tag{10}$$

where k_B represents the frequency of collisions among reacting molecules, E_a is the activation energy (kJ/µM) and *R* the constant of gases (0.008314 kJ.µM/K). Now, the parameter v_τ (analogous to rate constant *k*) of Eq. (8) can be substituted by Eq. (10) obtaining a simultaneous description of the kinetic profiles at all temperatures and AAPH concentrations by the following tri-variate model:

$$\overline{P}\left(t,T,P\right) = K\left\{1-\exp\left[-\left(\ln 2\right)^{1-\alpha}\left(\frac{2}{K\alpha}Be^{(-Ea/RT)}P\right)^{\alpha}\right]\right\} \tag{11}$$

The mathematical analysis of the averaged substrate protected $\overline{P}$ responses led to statistically significant description as a tri-variate function (lines of B1 and B2 plots from Figure 4), all the parameters where consistent and the correlation coefficients where always higher than 0.99 (Figure 4, B3 plot). The numerical values of the parameters from the tri-variate approach obtained are as follows: K=82.41±8.1 µM of Cr protected; E_a=79.44±15.2 kJ/µM; k_B=4.57x10^{+11}±1.1 x10^{+9}; and a=0.817±0.1. The correlation coefficient value was 0.9925 and the predicted and observed data didn't show any bias.

3.4.2. Kinetic assessment of the anti-oxidant capacity of trolox and pH

Previous authors (Bors, Michel & Saran, 1984b, Ordoudi & Tsimidou, 2006, Tubaro, Micossi & Ursini, 1996) have already studied the crocin bleaching in the presence of three antioxidants (caffeic acid, catechol and trolox) at various pHs (5.5 and 7.4), concluding that this variable causes significant differences in the first two cases but not in the case of trolox. In view of the impossibility to distinguish the effect of *pH* from that produced by an antioxidant in the Cr-AAPH system, as well as the risk of assessing antioxidant activities using a single time, we decided to revise that conclusion by studying the complete kinetics under the usual conditions (37ºC, 7.68 mM AAPH, 100 mM Briton buffer), combining 16 *pH* values and nine trolox concentrations (0-(19)-190 µM in the mixture reaction). All the kinetic results are presented in Figure A2 (Appendix section).

All the resulting standardized dose-response profiles of trolox for each *pH* could be described individually with accuracy by Eq. (8) (Table A1). Results presented in (dots of Figure 5, B1 plot) show a progressive reduction of the oxidation rate as the *pH* increases. Because the variable of pH does not affect the spontaneous discoloration rate of crocin, the effect must be attributed either to the inhibition of the AAPH degradation or to the capture of radicals from such a degradation. In any case, the increase of *pH* had an antioxidant-like effect. The interaction between the effects of trolox and the increase of *pH* produced a complex response, especially at *pHs* above 5.5, making complex the determination of the real capacity attributable to trolox. However, to describe the effect of *pH*, there is not a general formulation, compared to the effect of *T* applying the Arrhenius equation. In numerical terms, it can be observed that the P_m parameter varies asymptotically decreasing as a function of the *pH*, the v_τ parameter varies

linearly increasing and the shape parameter a remains constant. For its simplicity reasons we choose the model in Eq. (3) to describe such a behavior of P_m as follows:

$$P_m^{\bullet}(pH) = P_m^{\bullet} \exp\left[-\ln 2\left(pH/\tau_{Pm}\right)^{c_{Pm}}\right] \tag{12}$$

A linear approach without intercept was used to describe the behavior of v_τ as a function of the pH as follows:

$$v_\tau^{\bullet}(pH) = b \cdot pH \tag{13}$$

in which b is the slope of the linear relation. Therefore, by substituting the v_τ and P_m in Eq. (8) by Eq. (12) and (13) we describe in a tri-variate form, taken into consideration the time, antioxidant and the pH effect jointly as follows:

$$\overline{P}\left(t, A, pH\right) = P_m^{\bullet}\left\{1-\exp\left[-\left(\ln 2\right)^{1-a}\left(\frac{2A}{Ka}\left(v_\tau^{\bullet}\right)\right)^{a}\right]\right\} \tag{14}$$

The $\overline{P}$ described responses by Eq. (14) led to statistically significant description as a tri-variate function (Figure 5 plot B1), all the parameters where consistent (Figure 5, B2 plot) and the distribution of the predicted and observed values did not show any deviation or bias and the correlation coefficient higher than 0.99 (Figure 5, B3 plot). The numerical values of the parameters obtained and their estimations are as follows: $P_m^{\bullet}$=72.9±8.1 µM of Cr protected; τ_{Pm}=10.2±1.1 pH units; c_{Pm}=14.4±2.6; b=0.13±0.01µM Cr. µM trolox^{-1}/pH; a=1.17±0.1. The correlation coefficient value was 0.9925 and the predicted and observed data didn't show any bias.

4. DISCUSSION

The summary of kinetic profiles of an agent in area units standardized with respect the control represents a way of taking into account the kinetic profile but bypassing complex analytical expressions (Allison, Paultre, & Maggio, 1995). The new microplate methods allow obtaining effortless large temporal sampling with high accuracy. Its advantages are its simplicity and synthetism. However, the second advantage is also its biggest drawback due to the lack of possible interrelations between their values and some possible mechanistic consequences that have a clear practical interest.

Furthermore, the lack of an established mathematical model, to analyze the standardized *AUC* dose-responses and the traditional assumption of dose-response in linear terms, frequently lead to unreliable results and misinterpretations, making it extremely difficult to compare the obtained results. In our opinion, also shared by other authors (Murado & Vázquez, 2010; Özilgen & Özilgen, 1990; Prieto, Murado, Vázquez, & Curran, 2014; Terpinc, Bezjak, & Abramovič, 2009; Wardhani, Fuciños, Vázquez, & Pandiella, 2013), criterion that avoids a non-linear analysis of the standardized *AUC* values is a misleading simplification. We are aware that non-linear equations are slightly more complex than a linear one, but it is also much less deceiving. The model in Eq. (8) described accurately the antioxidant and pro-oxidant responses as a function of time and dose, because, it produces characterizing values of practical interest with high reproducibility. Additionally, in cases of complex responses such as samples with more than one effector, either opposite effects (*T vs.* pro-oxidant) or similar (antioxidant *vs. pH*), requires the use of equations to integrate their interaction effects or alternatively, their sum. In those types of

complex matrices, the application of a globalizing parameter, such as the area under the curve becomes very useful (Murado & Prieto, 2013). It allows to summarize the time part of the response in one global value and therefore, to quantify the dose responses with simple numerical values or graphical tools (Fang, Chen, Ke, & Lee, 2011; Fekedulegn et al., 2007). Thus, it is a very useful criteria (Bryant & Brvant, 1983; Wray, Yang, Goddard, & Visscher, 2010), in our opinion, is the most simple and complete approach when complex responses need to be studied and when the goal is to quantify.

The problems of using simple quantification alternatives for the area under the curve assessment criteria avoiding non-linear considerations are discussed in detail and a model is proposed for quantifying simultaneously anti- and pro-oxidant activities. Perhaps by using non-linear solutions to describe the oxidation process, we are also not helping to translate the results, because they may be related to the response itself, but at least we are able: 1) to describe precisely the kinetics detected in the many different reactions with antioxidants of very different nature; 2) to obtain reproducible characterizing values of practical interest, 3) to incorporate, if necessary, environmental variables that modify the process, 4) to infer mechanistic details which can be verified by other methods.

When the approach here discussed is applied to unroasted coffee beans extracts all the coffee samples promote the antioxidant capacity in both lipophilic and hydrophilic environments. The differences were narrow and were much higher in a hydrophilic environment than in a lipophilic one. Their AC potential capacity was greater than some of the standard antioxidants in terms of maximum capacity (P_m). When the analyses are based on the v_τ parameter, the coffee samples show between 6 to 40 times lower values than the standard antioxidants.

CONCLUSIONS

The combined use of a reproducible procedure and robust mathematical modeling produces consistent and meaningful criteria for the comparative characterization of any oxidation modifier, taking into account the dose-time-dependent behavior. The two characterizing parameters (P_m and v_τ) will vary in the presence of any M agent and, given their well-defined factual meanings regarding the oxidation, their combination have relevant meanings. Its application is simple, it provides parametric estimates which characterize the response, and it facilitates rigorous comparisons among the effects of different compounds and experimental approaches. Also, it enables the inclusion, if necessary, of environmental variables that modify the process, as well as the inference of mechanistic details that can be verified by other methods.

In this work, we have clearly demonstrated the capabilities of the model to discern the effects of several commercial agents providing useful information in the study of complex natural extracts containing components with variable degrees of modifier capacity. For all the assayed agents, statistically significant descriptions, with very accurate predictions, were provided by the model. For all experimental data tested, the calculated parameters were always statistically significant (Student's t-test, $\alpha = 0.05$), the equations were consistent (Fisher's F-test) and the goodness of fit coefficient of determination was higher than 0.98.

ACKNOWLEDGEMENTS

The authors wish to thank CSIC (Intramural project: 200930I183) and Ministerio de Ciencia e Innovación (project CTM2010-18411, co-financed with FEDER funds by European Union) for financial support. Miguel Angel Prieto Lage was awarded one grant from the JAE predoctoral program co-financed by the CSIC and European Social Fund (ESF). The authors want to express their gratitude to Araceli Menduiña Santomé for their professional work. We also want to thank

to the local manufacturer (CAFÉS CAMPINAS S. PAULO) who provided freely the coffee samples.

FIGURE CAPTIONS

Figure 1: Six illustrative cases illustrations simulated by Eq. (4). Each case is divided in two figures (a and b). The first one (a) shows the responses (*R*, from 0 to 1 units) for each of the kinetic profiles (0-200 time units) of increasing concentrations of an agent *M* (0-100 units). Note that the control profile has thicker line than the simulated increasing concentrations of *M*. The second one (b) shows the *RAU* values obtained. Parametric values of the simulations are presented in Table 1.

Figure 2: **A**, Shows the illustrative application of the model developed (Eq. (8)) to analyze the effect of the antioxidant of BHA and the pro-oxidant of Hb as a function of time and dose. Control series (●) and seven dilutions (○: 1/7, ▲: 2/7, △: 3/7, ■: 4/7, □: 5/7, ◆: 6/7, ◇: 7/7). **B**, **C** and **D**, shows the standardized $\overline{P}$ values obtained (dots ○) and the fittings to Eq. (8) (lines) for all the tested agents (pro-oxidants and antioxidants) for both complementary reactions (hydrophilic and lipophilic). All the kinetic dose-response results are shown the Figure A1 in the appendix section. Numerical results in Table 5 and dose ranges in material and methods section. **E**, numerical values of the parameters P_m and v_τ of Eq. (8) as assessment criteria. Parametric values of the fittings are presented in Table 2.

Figure 3: **A**, shows the dose-time dependency results of the five coffee samples (C1 to C5) using the two bleaching reactions (βCA and CA). Control series (●) and seven dilutions (○: 1/7, ▲: 2/7, △: 3/7, ■: 4/7, □: 5/7, ◆: 6/7, ◇: 7/7). **B** and **C**, shows the results of comparing by means of graphical and numerical criteria to the *AC* of commercial standards of antioxidants. Parametric values of the fittings are presented in Table 2.

Figure 4: Effect of temperature on bleaching of the crocin-AAPH system. **A:** kinetic data of four temperature values (● 32, ○ 37, ■ 40 and □ 45 ºC). **B1**: responses measured as relative area units in all combinations of *T* and trolox (● 32, ○ 37, ■ 40 and □ 45 ºC) fitted to Eq. (8) (lines). **B2**: effects of *T* on parameters of v_τ, the dots (○) are the individual result parameters obtained when Eq. (8) is used and lines when to Eq. (11) is applied. **B3**, correlation between observed and predicted values corresponding to tri-variate analysis. The numerical results for the dose response fittings with Eq. (8) for each temperature tested are summarized in Table A1.

Figure 5: Effect of *pH* (3.5-(0.5)-11.0) on bleaching of the crocin-AAPH-trolox system. **A**, kinetic data of four values of *pH* within the established range (points). Control series (●) and seven dilutions (○: 1/7, ▲: 2/7, △: 3/7, ■: 4/7, □: 5/7, ◆: 6/7, ◇: 7/7). All the kinetic results are presented in Figure A2 (Appendix section). **B1**, responses measured as relative area units in all combinations of *pH* and trolox (points ●) fitted to Eq. (14) (surface). **B2**: effects of *pH* on parameters P_m (●) and v_τ (○), the dots are the individual result parameters obtained when Eq. (8) is used and lines when to Eq. (14) is applied. **B3**, correlation between observed and predicted values corresponding to Figure B1. The numerical results for the dose response fittings with Eq. (8) for each pHs tested are summarized in Table A1.

TABLE CAPTIONS

Table 1: Parametric values used to recreate six simulated dose-time responses with the bi-variate model described in Eq. (5). Simulated cases are showed in Figure 1.

Table 2: Parametric estimates of equation (8) obtained after fitting the parametric results (P_m and v_τ parameters) for the crocin and β-Carotene bleaching affected by the specified agents. The confidence intervals (α=0.05) are in percentages. P_m values are in μM $\overline{P}$ and v_τ in μM $\overline{P}$/μg M.

APPENDIX FIGURE CAPTIONS

Figure A1: Kinetic data obtained for the individual time-dose-response analysis to the different antioxidant and pro-oxidant agents for the CA and βCA. Control series (●) and seven dilutions (○: 1/7, ▲: 2/7, △: 3/7, ■: 4/7, □: 5/7, ◆: 6/7, ◇: 7/7). Concentration ranges in Material and Methods section.

Figure A2: Kinetic data obtained for the individual time-dose-response analysis to the antioxidant agent of Trolox at different pHs (3.5-(0.5)-11.0) for the crocin bleaching reaction (CA). Control series (●) and seven dilutions (○: 1/7, ▲: 2/7, △: 3/7, ■: 4/7, □: 5/7, ◆: 6/7, ◇: 7/7). For all pHs series the Trolox concentrations ranges are 0-(15)-150 μM.

APPENDIX TABLE CAPTIONS

Table A1: Parametric estimates of equation (8) obtained after fitting the parametric results (P_m and v_τ parameters) for the crocin bleaching reaction (CA) affected by environmental conditions (T and pH). The part **A** shows the parametric fittings obtained for the individual dose-response analysis to the pro-oxidant agent AAPH for at different temperatures. The part **B** shows the parametric fittings obtained for the individual dose-response analysis to the antioxidant agent trolox for each pH tested. The confidence intervals (α=0.05) are in percentages.

REFERENCES

Allison, D., Paultre, F., & Maggio, C. (1995). The use of areas under curves in diabetes research. *Diabetes Care*, *18*(2), 245–250.

Almajano, M. P., Carbó, R., Delgado, M. E., & Gordon, M. H. (2007). Effect of pH on the antimicrobial activity and oxidative stability of oil-in-water emulsions containing caffeic acid. *Journal of Food Science*, *72*(5), C258–263.

Aruoma, O. (1999). Antioxidant actions of plant foods: use of oxidative DNA damage as a tool for studying antioxidant efficacy. *Free Radical Research*, *30*(6), 419–427.

Balk, J. M., Bast, A., & Haenen, G. R. M. M. (2009). Evaluation of the accuracy of antioxidant competition assays: incorrect assumptions with major impact. *Free Radical Biology & Medicine*, *47*(2), 135–144.

Bors, W., Michel, C., & Saran, M. (1984). Inhibition of the bleaching of the carotenoid crocin a rapid test for quantifying antioxidant activity. *Biochimica et Biophysica Acta*, *796*(3), 312–319.

Bryant, E. C., & Brvant, E. C. (1983). Area-under-the-curve analysis and other analysis strategies for repeated measures clinical trials, (1453).

Carlsen, M. H., Halvorsen, B. L., Holte, K., Bøhn, S. K., Dragland, S., Sampson, L., … Blomhoff, R. (2010). The total antioxidant content of more than 3100 foods, beverages, spices, herbs and supplements used worldwide. *Nutrition Journal*, *9*(3), 1–11.

Chatterjee, S., Poduval, T. B., Tilak, J. C., & Devasagayam, T. P. A. (2005). A modified, economic, sensitive method for measuring total antioxidant capacities of human plasma and natural compounds using Indian saffron (Crocus sativus). *Clinica Chimica Acta; International Journal of Clinical Chemistry*, *352*(1-2), 155–163.

Comuzzi, C., Polese, P., Melchior, A., Portanova, R., & Tolazzi, M. (2003). SOLVERSTAT: a new utility for multipurpose analysis. An application to the investigation of dioxygenated Co (II) complex formation in dimethylsulfoxide solution. *Talanta*, *59*(1), 67–80.

Dávalos, A. (2004). Extending applicability of the oxygen radical absorbance capacity (ORAC-fluorescein) assay. *Journal of Agricultural and Food Chemestry*, *52*(1), 48–54.

De Lean, A., Munson, P. J., & Rodbard, D. (1978). Simultaneous analysis of families of sigmoidal curves: application to bioassay, radioligand assay, and physiological dose-response curves. *The American Journal of Physiology*, *235*(2), E97–102.

Faller, A. L. K., & Fialho, E. (2009). The antioxidant capacity and polyphenol content of organic and conventional retail vegetables after domestic cooking. *Food Research International*, *42*(1), 210–215.

Fang, L., Chen, P., Ke, C., & Lee, E. (2011). Estimating area under the curve and relative exposure in a pharmacokinetic study with data below quantification limit. *Journal of Biopharmaceutical Statistics*, *21*(1), 66–76.

Fekedulegn, D. B., Andrew, M. E., Burchfiel, C. M., Violanti, J. M., Hartley, T. a, Charles, L. E., & Miller, D. B. (2007). Area under the curve and other summary indicators of repeated waking cortisol measurements. *Psychosomatic Medicine*, *69*(7), 651–659.

Frankel, E. N. (1994). Methods of evaluating food antioxidants: reply. *Trends in Food Science & Technology*, *51*, 56–57.

Garcıía-Alonso, M., Pascual-Teresa, S. de, Santos-Buelga, C., & Rivas-Gonzalo, J. C. (2004). Evaluation of the antioxidant properties of fruits. *Food Chemistry*, *84*(1), 13–18.

Gieseg, S. P., & Esterbauer, H. (1994). Low density lipoprotein is saturable by pro-oxidant copper. *FEBS Letters*, *343*(3), 188–194.

Gutteridge, J. M. C., & Halliwell, B. (2010). Antioxidants: Molecules, medicines, and myths. *Biochemical and Biophysical Research Communications*, *393*(4), 561–564.

Hamilton, R. (1997). Chemistry of free radicals in lipids. *Food Chemistry*, *60*(2), 193–199.

Huang, D., Ou, B., Hampsch-Woodill, M., Flanagan, J. A., & Deemer, E. K. (2002). Development and validation of oxygen radical absorbance capacity assay for lipophilic antioxidants using randomly methylated beta-cyclodextrin as the solubility enhancer. *Journal of Agricultural and Food Chemestry*, *50*(7), 1815–1821.

Huang, D., Ou, B., Hampsch-Woodill, M., Flanagan, J., & Prior, R. (2002). High-throughput assay of oxygen radical absorbance capacity (ORAC) using a multichannel liquid handling system coupled with a microplate fluorescence reader in 96-well format. *Journal of Agricultural and Food Chemistry*, *50*(16), 4437–4444.

Kemmer, G., & Keller, S. (2010). Nonlinear least-squares data fitting in Excel spreadsheets. *Nat.Protocols*, *5*(2), 267–281.

Laguerre, M., Lecomte, J., & Villeneuve, P. (2007). Evaluation of the ability of antioxidants to counteract lipid oxidation: existing methods, new trends and challenges. *Progress in Lipid Research*, *46*(5), 244–282.

Lu, M., Yuan, B., Zeng, M., & Chen, J. (2011). Antioxidant capacity and major phenolic compounds of spices commonly consumed in China. *Food Research International*, *44*(2), 530–536.

Madhava Naidu, M., Sulochanamma, G., Sampathu, S. R., & Srinivas, P. (2008). Studies on extraction and antioxidant potential of green coffee. *Food Chemistry*, *107*(1), 377–384.

Marco, G. J. (1968). A rapid method for evaluation of antioxidants. *Journal of the American Oil Chemists' Society*, *45*(9), 594–598.

Murado, M. A., & Prieto, M. A. (2013). Dose-Response Analysis in the Joint Action of Two Effectors. A New Approach to Simulation, Identification and Modelling of Some Basic Interactions. *PLoS ONE*, *8*(4), e61391.

Murado, M. A., & Vázquez, J. A. (2010). Mathematical model for the characterization and objective comparison of antioxidant activities. *Journal of Agricultural and Food Chemestry*, *58*(3), 1622–1629.

Naguib, Y. M. (2000). A fluorometric method for measurement of oxygen radical-scavenging activity of water-soluble antioxidants. *Analytical Biochemistry*, *284*(1), 93–98.

Özilgen, S., & Özilgen, M. (1990). Kinetic Model of Lipid Oxidation in Foods. *Journal of Food Science*, *55*(2), 498–501.

Pellegrini, N., Serafini, M., Salvatore, S., Del Rio, D., Bianchi, M., & Brighenti, F. (2006). Total antioxidant capacity of spices, dried fruits, nuts, pulses, cereals and sweets consumed in Italy assessed by three different in vitro assays. *Molecular Nutrition & Food Research*, *50*, 1030–1038.

Pérez-Jiménez, J., Arranz, S., Tabernero, M., Díaz- Rubio, M. E., Serrano, J., Goñi, I., & Saura-Calixto, F. (2008). Updated methodology to determine antioxidant capacity in plant foods, oils and beverages: Extraction, measurement and expression of results. *Food Research International*, *41*(3), 274–285.

Perva-Uzunalić, A., Škerget, M., Knez, Ž., Weinreich, B., Otto, F., & Grüner, S. (2006). Extraction of active ingredients from green tea (Camellia sinensis): Extraction efficiency of major catechins and caffeine. *Food Chemistry*, *96*(4), 597–605.

Prieto, M. A., Murado, M. A., & Vázquez, J. A. (2014). Quantification, characterization and description of synergy and antagonism in the antioxidant response. *Food Research International*, *60*, 218–229.

Prieto, M. A., Murado, M. A., Vazquez, J. A., Anders, Y., & Curran, T. P. (2013). A new microplate procedure for simultaneous assessment of lipophilic and hydrophilic antioxidants and pro-oxidants, using crocin and β-carotene bleaching methods in a single combined assay: Tea extracts as a case study. *Food Research International*, *53*(2), 836–846.

Prieto, M. A., Murado, M. A., Vázquez, J. A., & Curran, T. P. (2014). Analytical criteria to quantify and compare the antioxidant and pro-oxidant capacity in competition assays: The bell protection function. *Food Research International*, *60*, 48–58.

Prieto, M. A., Rodríguez-Amado, I., Vázquez, J. A., & Murado, M. A. (2012). β-Carotene assay revisited. Application to characterize and quantify antioxidant and prooxidant activities in a microplate. *Journal of Agricultural and Food Chemistry*, *60*(36), 8983–8993.

Prieto, M. A., Vázquez, J. A., & Murado, M. A. (2012). Comparison of several mathematical models for describing the joint effect of temperature and ph on glucanex activity. *Biotechnology Progress*, *28*(2), 372–381.

Prikler, S. (2009). *Advanced Excel for scientific data analysis* (2nd ed., pp. 159, 491). Robert de Levie Ed.

Pruessner, J. C., Kirschbaum, C., Meinlschmid, G., & Hellhammer, D. H. (2003). Two formulas for computation of the area under the curve represent measures of total hormone concentration versus time-dependent change. *Psychoneuroendocrinology*, *28*(7), 916–931.

Ragnarsson, J. O., & Labuza, T. P. (1977). Accelerated shelf-life testing for oxidative rancidity in foods–A review. *Food Chemistry*, *2*(4), 291–308.

Ramalakshmi, K., Rahath Kubra, I., & Jagan Mohan Rao, L. (2008). Antioxidant potential of low-grade coffee beans. *Food Research International*, *41*(1), 96–103.

Schisterman, E. F., Faraggi, D., Reiser, B., & Trevisan, M. (2001). Statistical inference for the area under the receiver operating characteristic curve in the presence of random measurement error. *American Journal of Epidemiology*, *154*(2), 174–179.

Stephen, S., Stevens, L., & Chaturvedi, N. (2000). TUTORIAL IN BIOSTATISTICS Repeated measures in clinical trials : simple strategies for analysis using summary measures. *Statistics in Medicine*, *19*, 861–877.

Terpinc, P., Bezjak, M., & Abramovič, H. (2009). A kinetic model for evaluation of the antioxidant activity of several rosemary extracts. *Food Chemistry*, *115*(2), 740–744.

Thomas, M. J., Chen, Q., Franklin, C., & Rudel, L. L. (1997). A comparison of the kinetics of low-density lipoprotein oxidation initiated by copper or by azobis (2-amidinopropane). *Free Radical Biology & Medicine*, *23*(6), 927–935.

Wardhani, D. H., Fuciños, P., Vázquez, J. A., & Pandiella, S. S. (2013). Inhibition kinetics of lipid oxidation of model foods by using antioxidant extract of fermented soybeans. *Food Chemistry*, *139*(1-4), 837–844.

Weibull, W., & Sweden, S. (1951). A statistical distribution function of wide applicability. *Journal of Applied Mechanics*, *18*(3), 293–297.

Wray, N. R., Yang, J., Goddard, M. E., & Visscher, P. M. (2010). The genetic interpretation of area under the ROC curve in genomic profiling. *PLoS Genetics*, *6*(2), e1000864.

FIGURES

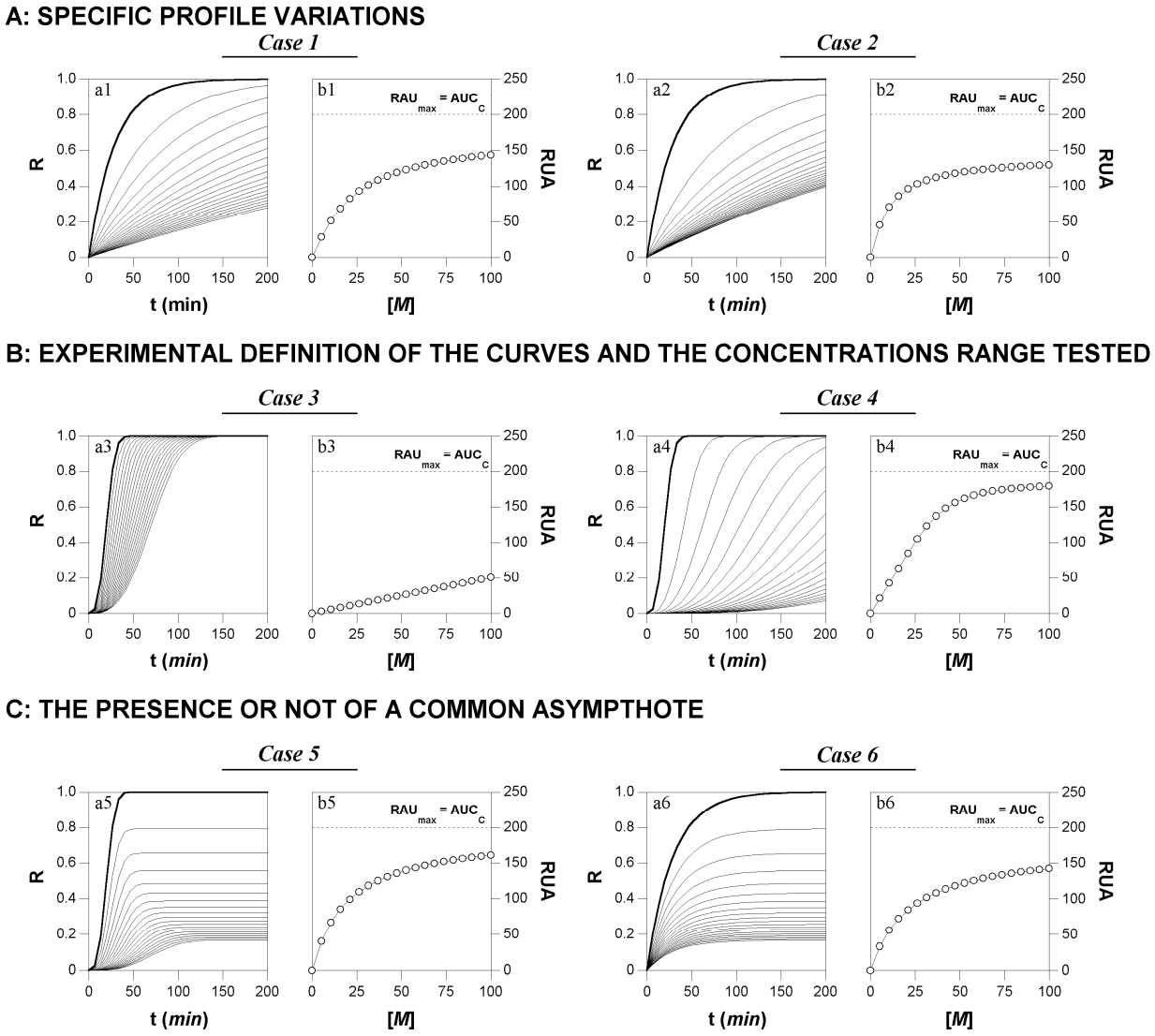

Figure 1: Six illustrative cases illustrations simulated by Eq. (4). Each case is divided in two figures (a and b). The first one (a) shows the responses (*R*, from 0 to 1 units) for each of the kinetic profiles (0-200 time units) of increasing concentrations of an agent *M* (0-100 units). Note that the control profile has thicker line than the simulated increasing concentrations of *M*. The second one (b) shows the *RAU* values obtained. Parametric values of the simulations are presented in Table 1.

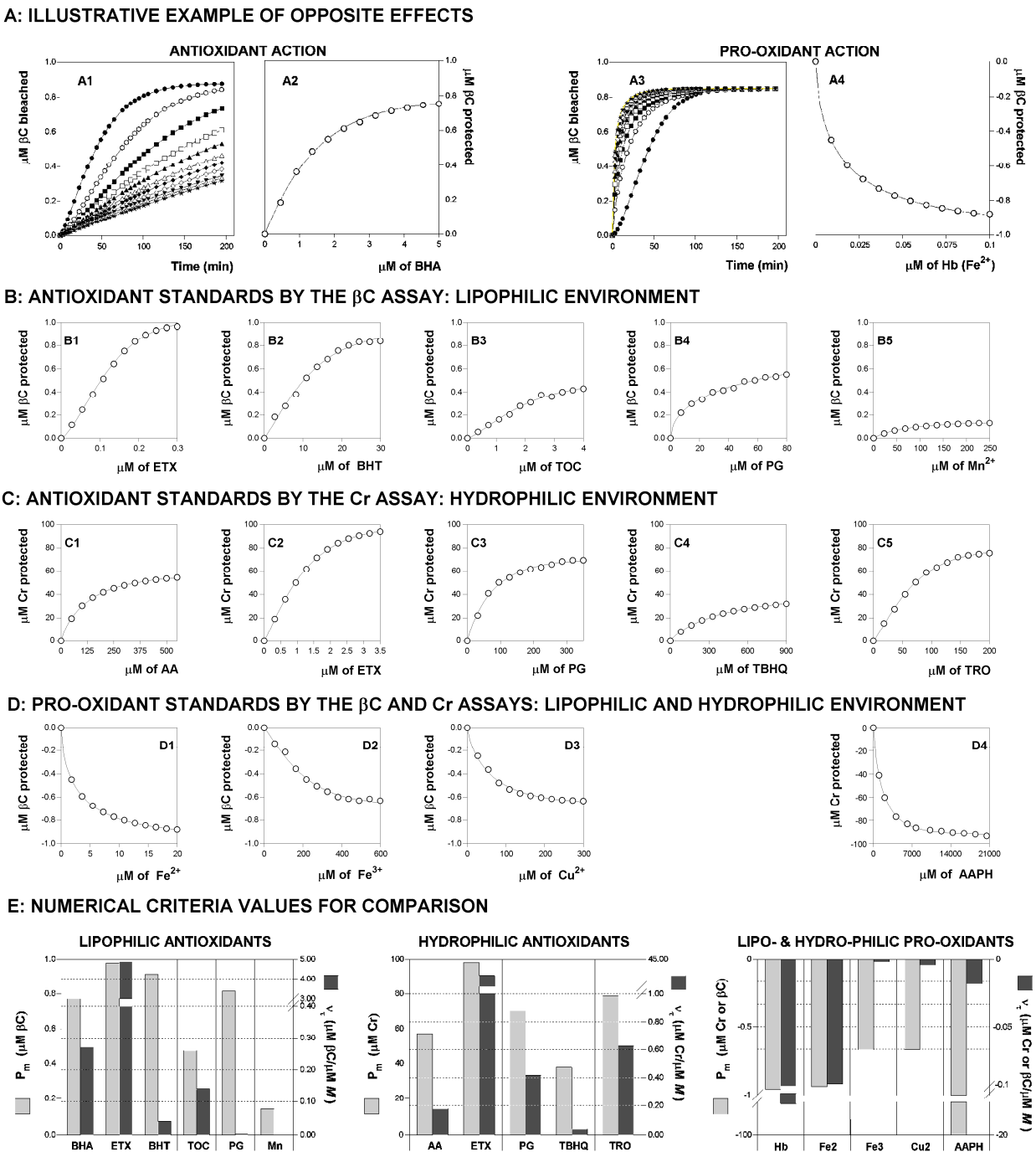

Figure 2: **A**, Shows the illustrative application of the model developed (Eq. (8)) to analyze the effect of the antioxidant of BHA and the pro-oxidant of Hb as a function of time and dose. Control series (●) and seven dilutions (○: 1/7, ▲: 2/7, △: 3/7, ■: 4/7, □: 5/7, ◆: 6/7, ◇: 7/7). **B**, **C** and **D**, shows the standardized $\overline{P}$ values obtained (dots ○) and the fittings to Eq. (8) (lines) for all the tested agents (pro-oxidants and antioxidants) for both complementary reactions (hydrophilic and lipophilic). All the kinetic dose-response results are shown the Figure A1 in the appendix section. Numerical results in Table 5 and dose ranges in material and methods section. **E**, numerical values of the parameters P_m and v_τ of Eq. (8) as assessment criteria. Parametric values of the fittings are presented in Table 2.

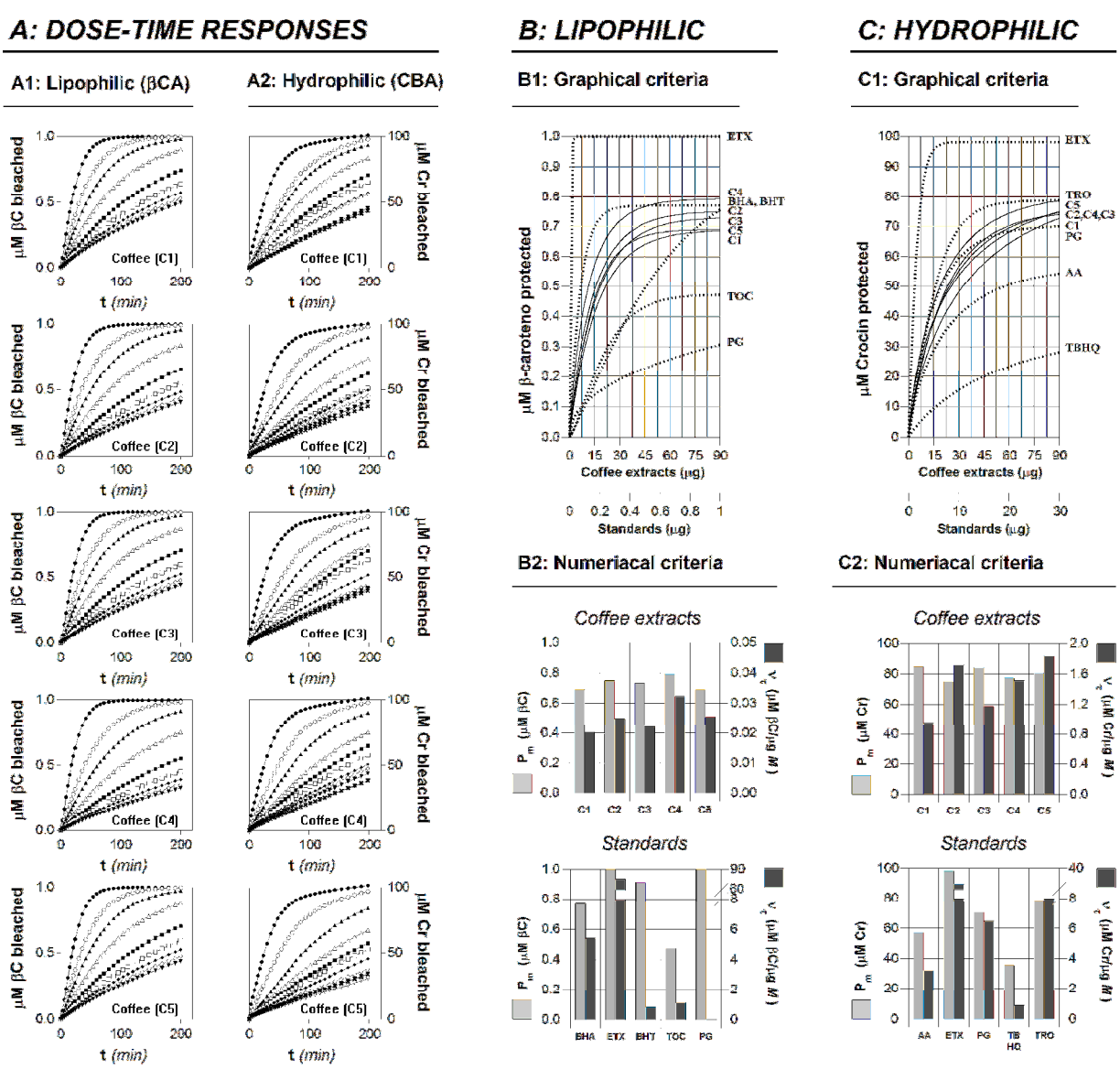

Figure 3: **A**, shows the dose-time dependency results of the five coffee samples (C1 to C5) using the two bleaching reactions (βCA and CA). Control series (●) and seven dilutions (○: 1/7, ▲: 2/7, △: 3/7, ■: 4/7, □: 5/7, ◆: 6/7, ◇: 7/7). **B** and **C**, shows the results of comparing by means of graphical and numerical criteria to the *AC* of commercial standards of antioxidants. Parametric values of the fittings are presented in Table 2.

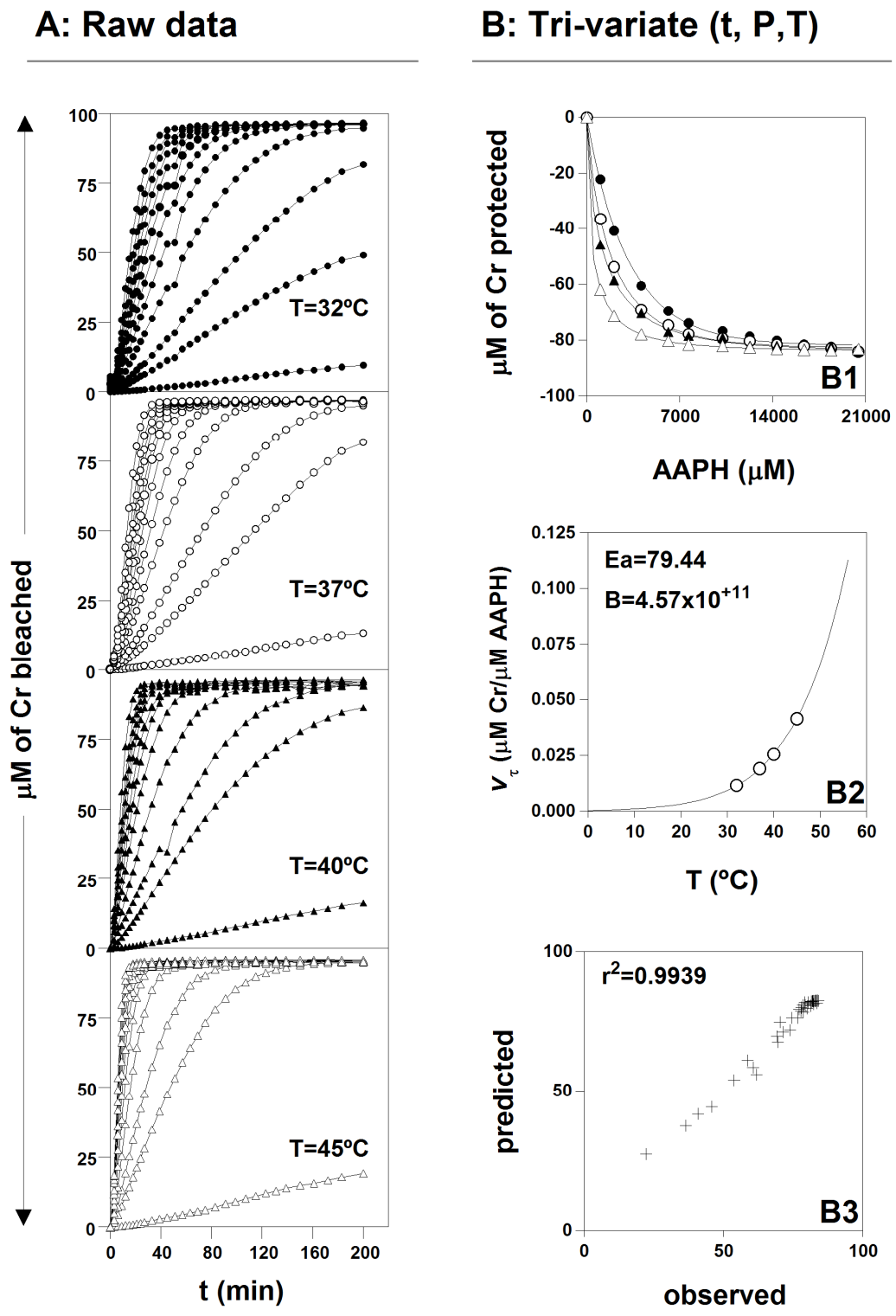

Figure 4: Effect of temperature on bleaching of the crocin-AAPH system. **A:** kinetic data of four temperature values (● 32, ○ 37, ■ 40 and □ 45 ºC). **B1**: responses measured as relative area units in all combinations of T and trolox (● 32, ○ 37, ■ 40 and □ 45 ºC) fitted to Eq. (8) (lines). **B2**: effects of T on parameters of v_τ, the dots (○) are the individual result parameters obtained when Eq. (8) is used and lines when to Eq. (11) is applied. **B3**, correlation between observed and predicted values corresponding to tri-variate analysis. The numerical results for the dose response fittings with Eq. (8) for each temperature tested are summarized in Table A1.

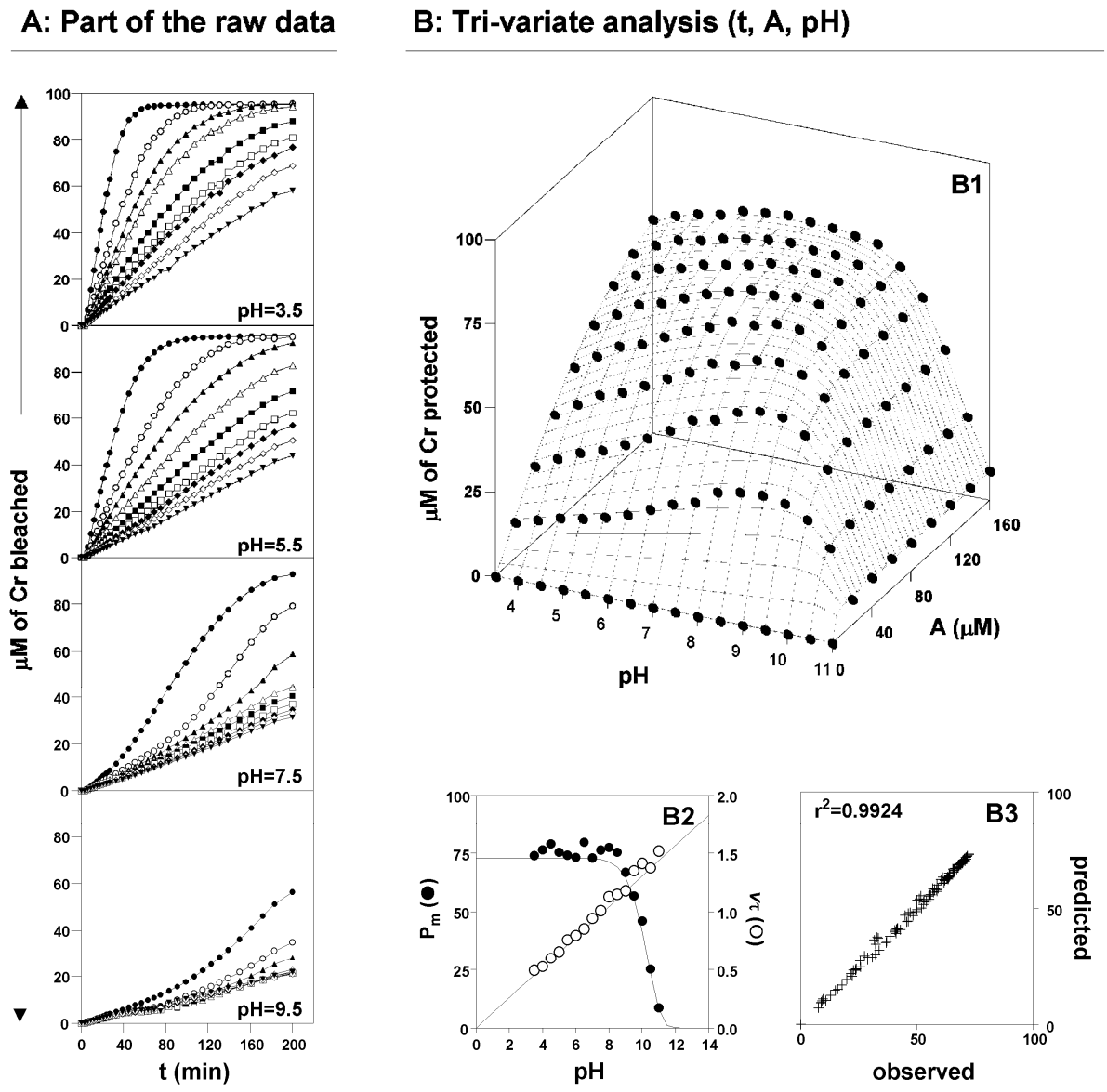

Figure 5: Effect of *pH* (3.5-(0.5)-11.0) on bleaching of the crocin-AAPH-trolox system. **A**, kinetic data of four values of *pH* within the established range (points). Control series (●) and seven dilutions (○: 1/7, ▲: 2/7, △: 3/7, ■: 4/7, □: 5/7, ◆: 6/7, ◇: 7/7). All the kinetic results are presented in Figure A2 (Appendix section). **B1**, responses measured as relative area units in all combinations of *pH* and trolox (points ●) fitted to Eq. (14) (surface). **B2**: effects of *pH* on parameters P_m (●) and v_τ (○), the dots are the individual result parameters obtained when Eq. (8) is used and lines when to Eq. (14) is applied. **B3**, correlation between observed and predicted values corresponding to Figure B1. The numerical results for the dose response fittings with Eq. (8) for each pHs tested are summarized in Table A1.

TABLES

Table 1: Parametric values used to recreate six simulated dose-time responses with the bivariate model described in Eq. (5). Simulated cases are showed in Figure 1.

	KINETIC PARAMETERS			**DOSE-RESPONSE PARAMETERS**					
				K modifiers		***τ modifiers***		***α modifiers***	
	K	τ	α	m_K	n_K	m_τ	n_τ	m_α	n_α
Case 1	1.00	20.00	1.00	--	--	0.200	--	--	--
Case 2	1.00	20.00	1.00	--	--	0.400	0.020	--	--
Case 3	1.00	20.00	3.00	--	--	0.025	--	--	--
Case 4	1.00	20.00	3.00	--	--	0.200	--	--	--
Case 5	1.00	20.00	3.00	--	0.050	0.025	--	--	--
Case 6	1.00	20.00	1.00	--	0.050	0.025	--	--	--

Table 2: Parametric estimates of equation (8) obtained after fitting the parametric results (P_m and v_τ parameters) for the crocin and β-Carotene bleaching affected by the specified agents. The confidence intervals (α=0.05) are in percentages. P_m values are in μM $\overline{P}$ and v_τ in μM $\overline{P}$/μg M.

	P_m	v_τ	α	r^2
A: βCA				
BHA	0.771±7.6	5.419±1.1	1.04±5.6	0.9990
ETX	1.000±19.2	75.99±0.3	1.50±12.8	0.9982
BHT	0.914±7.2	0.823±8.0	1.18±5.6	0.9950
TOC	0.473±8.8	1.122±3.7	1.32±3.1	0.9936
PG	1.000±7.5	0.047±15.9	0.50±15.2	0.9964
Mn^{2+}	0.141±25.4	0.059±15.4	0.86±10.3	0.9998
Hb	-0.957±0.3	-18.509±4.1	0.58±3.3	0.9999
Fe^{2+}	-0.939±2.1	-0.2980±5.0	0.60±4.7	0.9999
Fe^{3+}	-0.670±5.4	-0.0018±18.6	1.14±8.7	0.9937
Cu^{2+}	-0.669±0.8	-0.0044±6.1	0.77±3.2	0.9957
C1	0.689±7.9	0.0203±26.4	0.98±39.1	0.9998
C2	0.752±24.1	0.0249±59.7	0.93±57.6	0.9996
C3	0.732±10.5	0.0220±36.3	0.96±23.8	0.9997
C4	0.793±32.8	0.0322±69.7	0.90±81.2	0.9994
C5	0.690±9.2	0.0255±13.4	1.06±9.2	0.9986
B: CA				
AA	57.13±1.0	0.177±2.3	0.81±9.7	0.9998
ETX	98.23±2.2	42.66±0.1	1.15±8.6	0.9998
PG	70.56±1.1	0.417±1.8	0.93±20.9	0.9961
TBHQ	37.91±0.8	0.040±7.5	0.84±29.2	0.9996
TRO	78.74±0.5	0.625±0.1	1.20±12.8	0.9992
AAPH	-95.82±*9.1*	-0.019±*8.2*	0.62±*1.5*	0.9991
C1	84.85±9.1	0.957±28.6	0.77±24.9	0.9962
C2	75.26±8.0	1.720±9.3	0.97±50.9	0.9990
C3	83.99±5.0	1.179±8.6	0.72±57.5	0.9963
C4	77.50±8.2	1.516±6.3	0.88±49.5	0.9986
C5	80.77±15.0	1.839±17.7	0.84±16.8	0.9938

APPENDIX

APPENDIX FIGURES

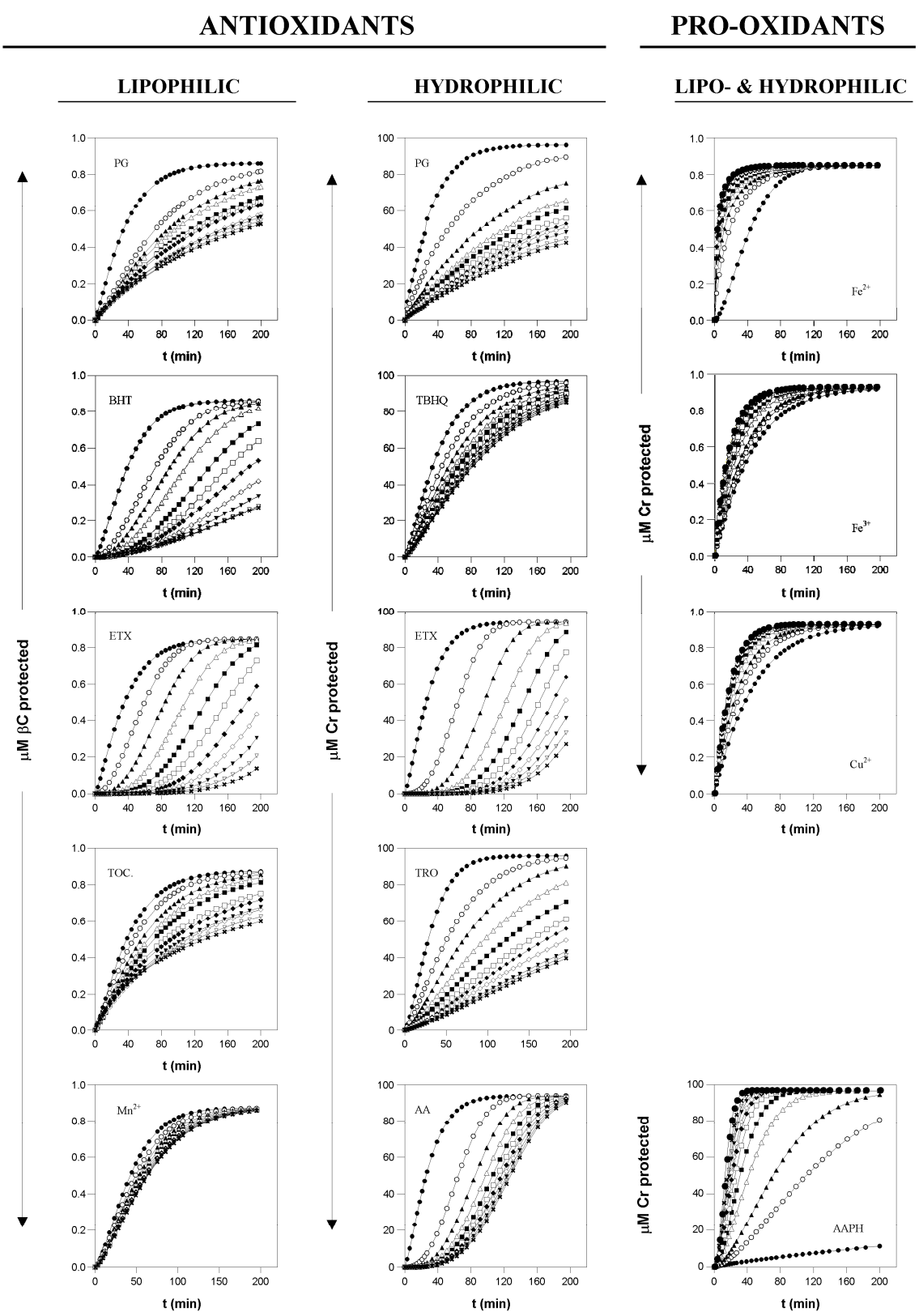

Figure A1: Kinetic data obtained for the individual time-dose-response analysis to the different antioxidant and pro-oxidant agents for the CA and βCA. Control series (●) and seven dilutions (○: 1/7, ▲: 2/7, △: 3/7, ■: 4/7, □: 5/7, ◆: 6/7, ◇: 7/7). Concentration ranges in Material and Methods section.

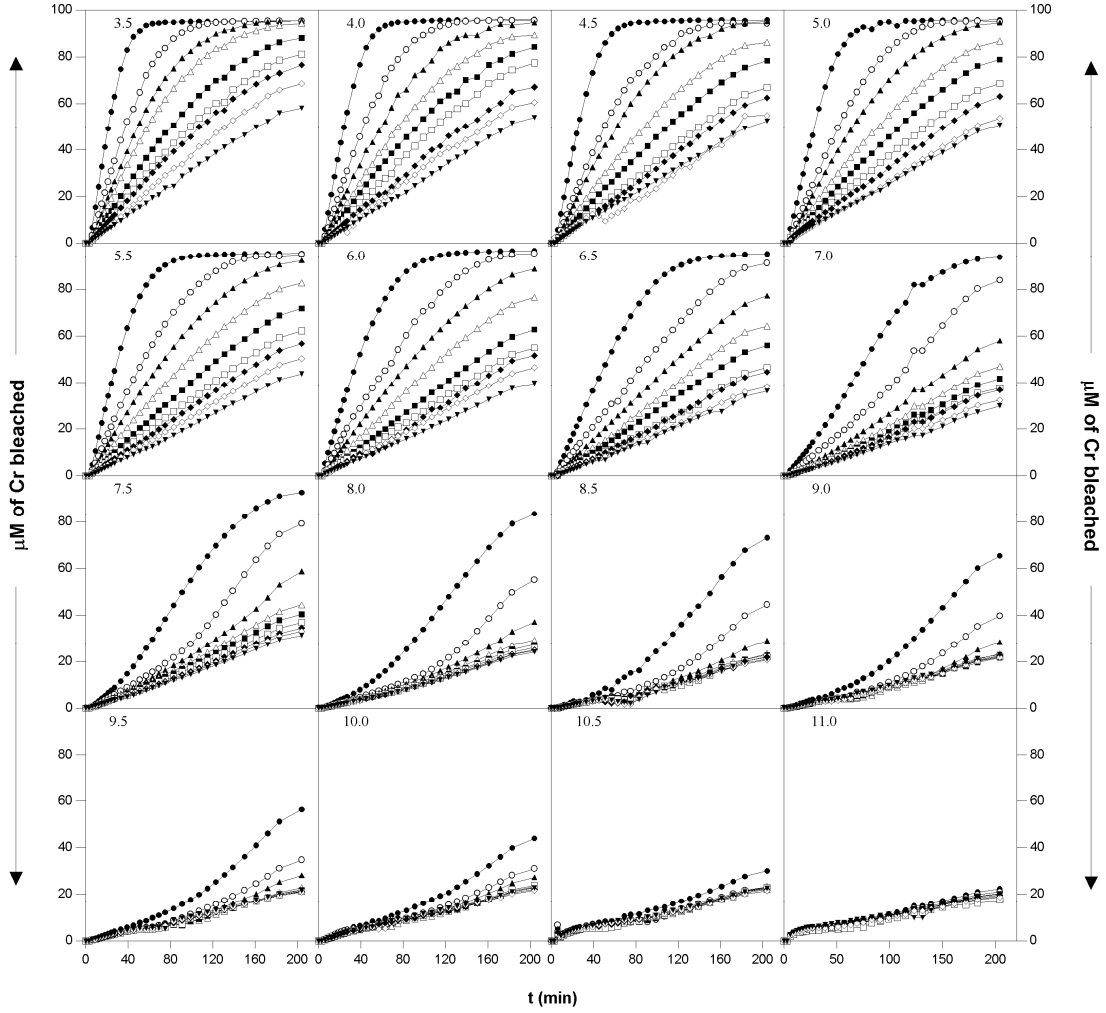

Figure A2: Kinetic data obtained for the individual time-dose-response analysis to the antioxidant agent of trolox at different pHs (3.5-(0.5)-11.0) for the crocin bleaching reaction (CA). Control series (●) and seven dilutions (○: 1/7, ▲: 2/7, △: 3/7, ■: 4/7, □: 5/7, ◆: 6/7, ◇: 7/7). For all pHs series the Trolox concentratios ranges are 0-(15)-150 µM.

APPENDIX TABLES

Table A1: Parametric estimates of equation (8) obtained after fitting the parametric results (P_m and v_τ parameters) for the crocin bleaching reaction (CA) affected by environmental conditions (T and pH). The part **A** shows the parametric fittings obtained for the individual dose-response analysis to the pro-oxidant agent AAPH for at different temperatures. The part **B** shows the parametric fittings obtained for the individual dose-response analysis to the antioxidant agent trolox for each pH tested. The confidence intervals (α=0.05) are in percentages.

	P_m	v_τ	a	r^2
A: AAPH AT DIFFERENT TEMPERATURES (ºC)				
32.0	82.03±0.5	0.0115±8.1	0.81±1.8	0.9998
37.0	82.83±3.2	0.0191±9.2	0.79±1.2	0.9996
40.0	83.75±2.1	0.0256±1.0	0.80±2.5	0.9997
45.0	83.78±8.0	0.0413±9.0	0.80±5.1	0.9994
B: TROLOX AT DIFFERENT pH				
3.50	74.64±8.0	0.464±0.2	1.26±14.8	0.9990
4.00	77.69±3.8	0.529±6.8	1.27±6.8	0.9982
4.50	74.17±9.3	0.637±18.3	1.19±16.3	0.9950
5.00	79.25±14.5	0.674±21.1	1.18±18.6	0.9936
5.50	74.79±6.5	0.753±10.8	1.25±28.1	0.9964
6.00	79.65±2.1	0.825±4.7	1.20±3.7	0.9998
6.50	74.07±2.7	0.883±4.4	1.23±3.9	0.9958
7.00	72.76±7.3	0.965±4.1	1.20±3.3	0.9999
7.50	77.02±2.1	1.046±5.0	1.20±4.7	0.9999
8.00	72.54±5.4	1.062±18.6	1.19±8.7	0.9937
8.50	72.55±7.8	1.159±6.1	1.24±3.2	0.9957
9.00	70.29±2.8	1.176±1.1	1.23±8.2	0.9998
9.50	58.62±7.9	1.365±26.4	1.29±9.1	0.9998
10.00	45.27±24.1	1.318±59.7	1.19±7.6	0.9996
10.50	26.23±1.5	1.420±36.3	1.25±2.8	0.9997
11.00	9.03±9.2	1.552±69.7	1.28±8.2	0.9994